Single enzyme nanoparticles with improved biocatalytic activity through protein entrapment in a surfactant shell

Dylan L. Atkins,[1,2] J. Rodrigo Magana,[1,2] Christian C. M. Sproncken,[1,2] Jan C.M. van Hest,[2,3] Ilja K. Voets[1,2*]

Laboratory of Self-Organizing Soft Matter, Department of Chemical Engineering and Chemistry, Eindhoven University of Technology, 5600 MB Eindhoven, the Netherlands.

Institute for Complex Molecular Systems, Department of Chemical Engineering and Chemistry, Eindhoven University of Technology, 5600 MB Eindhoven, the Netherlands.

Laboratory of Bio-Organic Chemistry, Department of Chemical Engineering and Chemistry, Eindhoven University of Technology, 5600 MB Eindhoven, the Netherlands.

*Corresponding author

Supplementary Information

Continuum electrostatics calculations

Computations were performed using the PDB2PQR[5] webserver and Adaptive Poisson-Boltzmann Solver (APBS).[6] The associated pdb file for HEWL (1dpx)[35] was used for calculations, whilst mutagenesis of the solvent-accessible Asp/Glu residues was performed by approximating these surface modifications as Lys residues in PyMOL. Initally, calculations were performed using an AMBER forcefield and protonation states were assigned for pH 6.5. Default input parameters were subsequently used for computation for determination of the surface electrostatic parameters of HEWL and cHEWL.

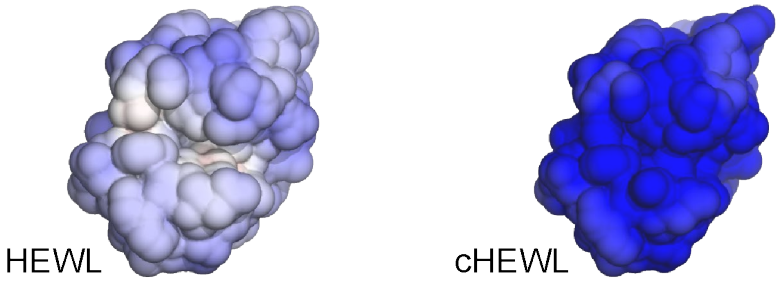

Figure S1. Map of surface electrostatic potential for hen egg-white lysozyme (HEWL) and the cationic supercharged variant (cHEWL). Surface electrostatic potentials are contour colored (red to blue) from -10 to +10 kT e^{-1}. The color map clearly indicates that modication of the solvent-accessible Asp/Glu residues on HEWL to yield cHEWL results in high cationic charge density distriuted reasonably evenly accross the protein surface.

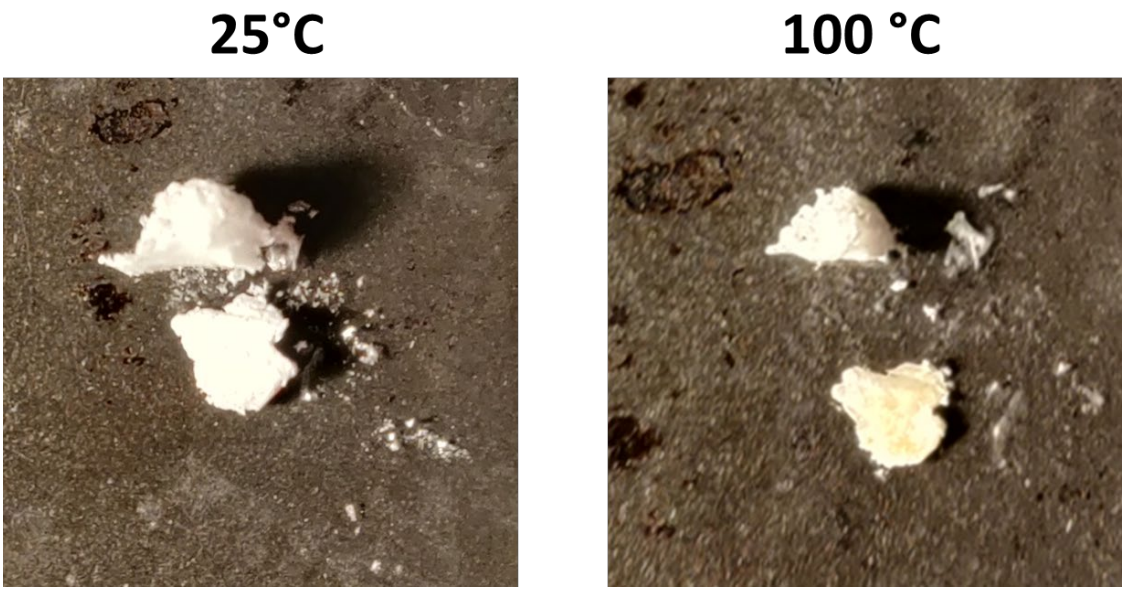

Figure S2. Representative photographs of a freeze-dried mixture of protein:surfactant (70:30 ratio) at 25 °C and 100 °C

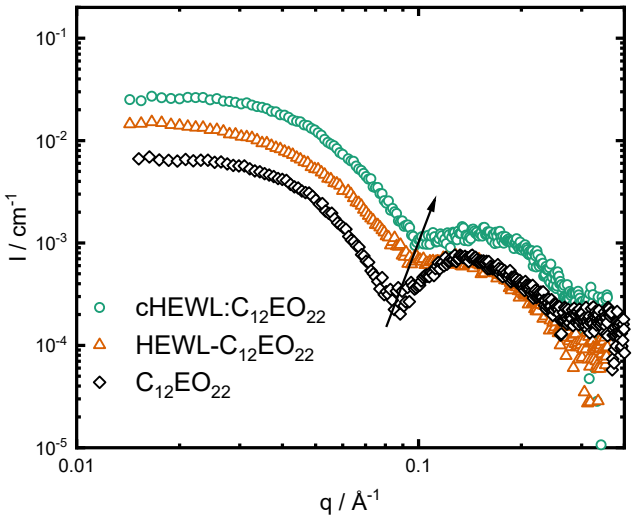

Figure S3. (a) SAXS profiles comparison between cHEWL:$C_{12}EO_{22}$ (circles), HEWL-$C_{12}EO_{22}$ (triangles), and $C_{12}EO_{22}$ micelles (diamonds).

Secondary structure deconvolution

Table S1. Structural contents of native and modified proteins resolved through deconvolution of circular dichroism (CD) spectroscopy traces.

	HEWL	**cHEWL**	**HEWL-$C_{12}EO_{10}$**	**HEWL-$C_{12}EO_{22}$**	**cHEWL:$C_{12}EO_{10}$**	**cHEWL:$C_{12}EO_{22}$**
α-Helix	37	36	30	32	33	29

β-Sheet	17	18	21	19	16	18
Turn	19	19	18	19	17	22
Disordered	27	27	31	30	34	31

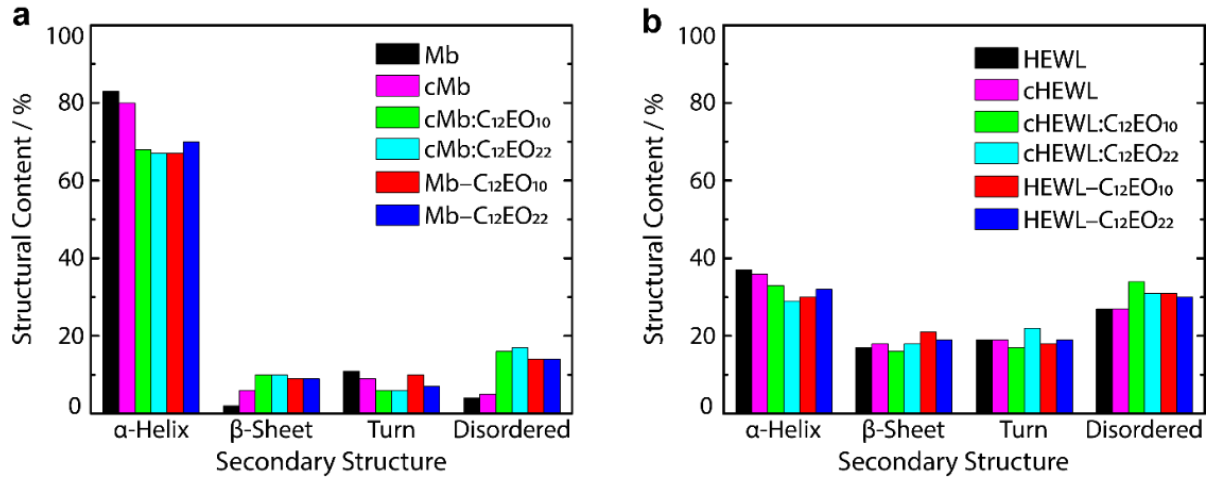

Figure S3. (a) Secondary structure deconvolution from circular dichroism (CD) spectroscopy traces indicating the structural contents of native Mb (black), cMb (pink), cMb:$C_{12}EO_{10}$ (green), cMb:$C_{12}EO_{22}$ (cyan), Mb-$C_{12}EO_{10}$ (red), and Mb-$C_{12}EO_{22}$ (blue). (b) Structural contents of HEWL (black), c HEWL (pink), cHEWL:$C_{12}EO_{10}$ (green), cHEWL:$C_{12}EO_{22}$ (cyan), HEWL-$C_{12}EO_{10}$ (red), and HEWL-$C_{12}EO_{22}$ (blue). Secondary structure deconvolution shows high degrees of structural retention independent of surfactant conjugation approach.

Kinetics assays using bacterial substrate

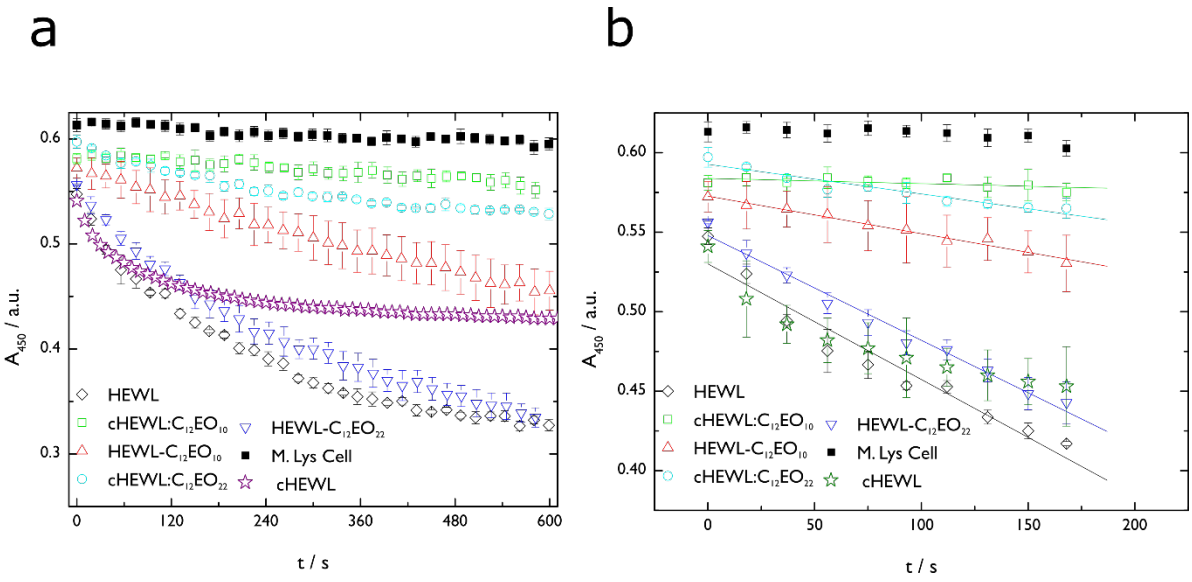

Figure S4. (a) UV-vis spectroscopy traces for the lysis of *M. lys.* whole bacterial cells followed at 450 nm (A_{450}) with respect to time for native HEWL (black diamonds), cHEWL:$C_{12}EO_{10}$ (green squares), HEWL-

$C_{12}EO_{10}$ (red upward triangles), cHEWL:$C_{12}EO_{22}$ (cyan circles), and HEWL-$C_{12}EO_{22}$ (blue downward triangles). A control experiment containing *M. lys.* whole cells but in absence of HEWL is indicated (black closed squares). (b) Corresponding inset of the first 180 s of assays indicating the linear fits obtained, and from which activity retention is approximated for HEWL variants. Error bars indicate the standard deviation obtained from three independent assays.